CdSe nanowires with illumination-enhanced conductivity: Induced dipoles, dielectrophoretic assembly, and field-sensitive emission

Ronghui Zhou and Hsueh-Chia Chang[a),b)]
Department of Chemical and Biomolecular Engineering, University of Notre Dame, Notre Dame, Indiana 46556

Vladimir Protasenko and Masaru Kuno[a),c)]
Department of Chemistry and Biochemistry, University of Notre Dame,Notre Dame, Indiana 46556

Amol Kumar Singh, Debdeep Jena, and Huili (Grace) Xing[a),d)]
Department of Electrical Engineering, University of Notre Dame,Notre Dame, Indiana 46556

(Received 18 September 2006; accepted 24 January 2007; published online 6 April 2007)

Positive ac dielectrophoresis (DEP) is used to rapidly align ensembles of CdSe semiconductor nanowires (NWs) near patterned microelectrodes. Due to their large geometric aspect ratio, the induced dipole of the wires is proportional to their conductivity, which can be drastically enhanced under super-band-gap illumination by several orders of magnitude, with a corresponding increase in the wire DEP mobility. This optical enhancement of conductivity occurs because of the generation of mobile electrons and holes and is verified by a photocurrent measurement. The linear nanowire alignment exhibits a high degree of fluorescent polarization anisotropy in both absorption and emission. An unexpected observation is a reversible, factor of ~4, electric-field-induced, and frequency-dependent enhancement of the nanowire emission near 10 Hz. Such illumination-sensitive, field-enhanced, and frequency-dependent alignment and emission phenomena of NWs suggest an electrical-optical platform for fabricating CdSe nanowire devices for polarization-sensitive photodetection and biosensing applications. © *2007 American Institute of Physics*. [DOI: 10.1063/1.2714670]

INTRODUCTION

A great deal of research in nanostructures (nanocrystals and nanowires) has focused on demonstrating that these materials can be employed in devices such as field-effect transistors, photodetectors, and light-emitting diodes, in a manner akin to uses of conventional bulk solids.[1] At the same time, solution-based semiconductor nanostructures such as CdSe nanowire[2,3] (NW) colloidal quantum dots (Qds) [or nanocrystals (NCs)][4] offer added degrees of freedom, distinct from bulk behavior. In principle, these properties can be exploited and thus represent a paradigm shift for device applications. For example, nanostructures suspended in a dielectric medium can be reversibly moved in and out of solution using external stimuli,[5] forming conductive as well as optically active networks in precisely defined regions of a substrate.[6] This controllable self-assembly, coupled to size-dependent optical and electrical properties,[2] opens up powerful fabrication techniques for nanostructure-based devices.

Among low dimensional materials, semiconductor NWs exhibit strong photoconductivity,[7,8] as well as visible fluorescence,[9,10] due to their direct band gap nature. They do not suffer from problems associated with admixtures of metallic and semiconducting species, commonly encountered in carbon nanotubes (CNTs).[11] Furthermore, they can be made to emit in the visible by suitably modifying the size and shape of the nanostructure.[12] These dependencies have been theoretically modeled for quasi-one-dimensional systems such as semiconductor nanorods (NRs).[13]

Because CdSe NWs have the same crystal structure as corresponding NRs and QDs, albeit with larger aspect ratios, they have similar optical properties. However, significant differences between NWs and NRs (or NCs) exist, including the presence of one-dimensional (1D) excitons,[14,15] potential dielectric contrast effects,[14,15] enhanced 1D exciton binding energies,[15] variations in the effective fluorescence quantum yield, and strong changes in the density of states underlying the linear absorption. An additional difference, important for field-directed nanocircuit assembly but seldom noted, is the fact that NWs possess potentially significant induced and/or permanent dipole moments due to their highly anisotropic shapes. In this respect, NW aspect ratios can reach values of 10^3 or more due to their narrow diameters (<10 nm) and micron long lengths.[2,3] When coupled to the presence of a polar wurtzite (WZ) phase, CdSe NWs, grown along the *c* axis (⟨0001⟩ direction), can therefore behave as giant electrets in the absence of an external electric field. More specifically, hexagonal CdSe possesses a spontaneous polarization on the order of $P \sim 0.2–0.6\ \mu C/cm^2$. [Actual literature estimates are $P=0.19$,[16] $P=0.42$,[17] and $P=0.6\ \mu C/cm^2$ (Ref. 18).] These numbers are comparable to some of the largest values seen in wurtzite III-V semiconductors such as GaN ($\sim 3\ \mu C/cm^2$).[19] Even in CdSe NWs with admixtures of wurtzite and zinc blende (ZB) as well as twinned ZB

[a)]Authors to whom correspondence should be addressed.
[b)]Electronic mail: hchang@nd.edu
[c)]Electronic mail: mkuno@nd.edu
[d)]Electronic mail: hxing@nd.edu

sections,[3] many smaller dipoles might exist within individual wurtzite links (all aligned end to end along the NW length), giving rise to a significant permanent dipole.

Assembly of nanocircuitry involving NWs requires a mechanism to manipulate and assemble the NWs—a force must be imparted on the NWs to direct their assembly into functional circuits. The permanent dipoles offer such a mechanism by generating an electric torque on the NW in an applied field that can align them along the field line. The aligned NWs would not experience a net force in a spatially uniform field but will suffer one in a nonuniform dc field. For NWs, the resulting mobility is in the direction of the high field region, known as positive dc dielectrophoresis (DEP). In a nonuniform ac field, on the other hand, there would be no force on the aligned permanent dipoles.

Other than permanent dipoles, NWs are also endowed with a large polarizability such that they exhibit high induced dipoles in an electric field. For NWs and CNTs that are more conducting than the medium, induced ac dipoles are parallel to the field. As they reverse polarity with the ac field, a spatially nonuniform ac field can impart a net (time-averaged) Maxwell force on the NWs and CNTs such that they exhibit a net motion in the direction of the higher field (positive DEP). This ac dielectrophoresis phenomenon is preferred over dc dielectrophoresis of permanent dipoles (or dc induced dipoles), as high frequency ac fields do not carry a net current and hence do not produce undesirable Faradic products such as bubbles and contaminating ions during the assembly.

The permanent and induced dipoles could further produce dipolar or induced-dipolar interaction to assemble the NW into aligned structures. A promising nanocircuitry fabrication technique is hence to sort and manipulate NWs and CNTs dielectrophoretically with sequentially activated local fields, sustained by micro-fabricated ac microelectrodes or microchannels, such that the NWs assemble into complex nanonetworks of field-effect transistors, photoemitters, and sensors. Although a functional nanocircuitry has yet to be assembled in this manner, simple array assembly has been demonstrated in the alignment of metal NWs by dielectrophoresis.[20] The approach thus complements other potential fabrication techniques for nanowires, including Langmuir-Blodgett[21–23] and microfluidic alignment.[24,25] There are more reports of CNT assembly and alignment by DEP,[24–28] although the application of CNTs is still severely limited by their nonuniform band gap in the mixture (i.e., metallic versus semiconducting tubes with a range of band gap).

Unlike spherical nanocolloids whose DEP mobility is insensitive to particle/medium conductivity, the large NW aspect ratio also endows NWs with a DEP mobility that is proportional to the NW conductivity. This is particularly pertinent in the present study, as we shall demonstrate that, under super-band-gap illumination, charge carriers can be generated in the CdSe NWs such that its conductivity can increase by orders of magnitude. Thus, their DEP mobility is greatly enhanced. Moreover, we shall demonstrate that the same illumination-generated carriers can enhance bundling of NWs, which has profound implications in sensing applications. For example, ensembles of aligned NWs and CNTs have been used to promote the capture of pathogens such as bacteria[24] both at the ensemble and single particle levels. In this respect, the illumination-enhanced field at the end of the NW can promote pathogen-NW dipole-induced "docking" as supported by our earlier work on the DEP trapping of CNTs and CNT/bacteria mixtures.[24] Underlying this phenomenon is an induced dipole-induced dipole attraction with an interaction potential energy of ~50 kT as calculated from their dielectrophoretic velocity. Furthermore, given the direct band gap emission of the wires, changes in their emission intensity after pathogen docking may provide an alternative means of sensing apart from standard conductivity measurements.[1] The illumination-enhanced assembly of NW under an applied ac electric field, their fluorescence behavior both in the presence and absence of the field as well as their corresponding transport properties are therefore of practical interest for aforementioned potential applications.[29]

These interesting electric-optical properties of CdSe NWs during and after assembly suggest a potentially powerful electrical-optical fabrication platform for sensing nanocircuitries based on CdSe NWs. Our investigation of this approach involves visual confirmation of NW alignment with subsequent bright field and epifluorescence measurements. The ac dielectrophoretic velocity of semiconducting NWs is shown to be enhanced using super-band-gap illumination by three orders of magnitude higher than that due to pure dielectric polarization and migration of intrinsic charge carriers on the NW, depending on the illumination intensity. As expected, a corresponding increase in DEP mobility and assembly speed is observed. These rapidly aligned assemblies exhibit strong polarization anisotropies in both the absorption and emission. As previously emphasized, an unexpected enhancement of the NW emission, by a factor of ~4, is observed in the presence of an electric field. This behavior is unexpected as such a field is generally anticipated to quench any emission due to the reduced spatial overlap between electron and hole wave functions,[30] though it is possible that enhanced 1D exciton binding energies could suppress this effect.[15]

EXPERIMENTS

Narrow diameter (<10 nm) CdSe NWs with lengths between 1 and 10 μm were synthesized using a seeded solution approach.[2,3] The asymmetric growth is catalyzed in the presence of mild coordinating surfactants such as trioctylphosphine oxide (TOPO), using low melting, bimetallic Au/Bi core/shell nanoparticles (NPs). Such bimetallic Au/Bi catalysts have also been used in the solution phase synthesis of other NWs including PbSe (Ref. 31) and more recently CdTe.[32] As a representative low resolution transmission electron microscope (TEM) micrograph shown in Fig. 1(a), these CdSe NWs have diameters between 7 and 10 nm and lengths exceed 1 μm (>10 μm in some cases). Corresponding diameter distributions are on the order of 25%. Figure 1(b) shows that the wires are crystalline and uniform, with intrawire diameter distributions between 3% and 6%.[3,9] Although the high resolution micrograph in Fig. 1(b) shows

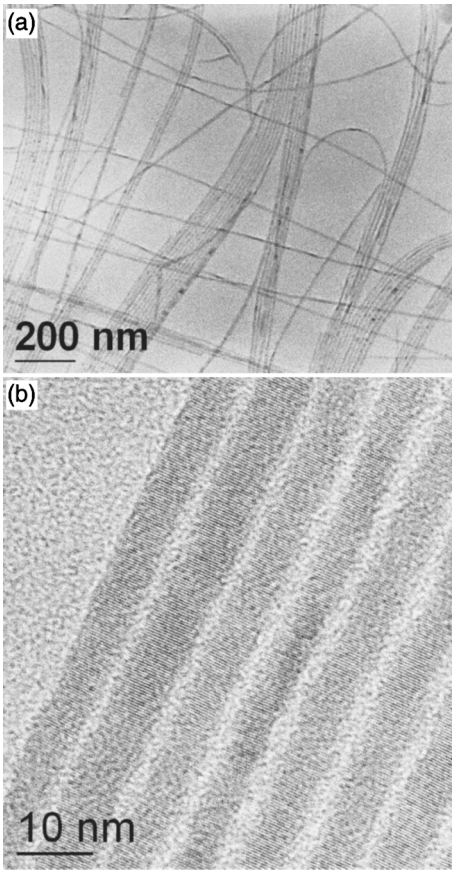

FIG. 1. (a) Low and (b) high resolution TEM images of CdSe NWs.

that the wires are crystalline, it hides the fact that individual NWs exhibit admixtures of zinc blende and wurtzite phases. This can be seen in properly oriented (⟨110⟩ zone) wires, as described in more detail in Ref. 3. Nanowires with branched morphologies can also be made using variations of the approach, involving different initial metal to chalcogen precursor ratios.[3] In all cases, NW surfaces are passivated with organic ligands such as trioctylphosphine oxide, trioctylphosphine, and octanoic acid. As a consequence, the recovered NWs can be resuspended in common organic solvents such as toluene or chloroform. All our experiments are performed with a chloroform solvent. Despite the solvent's low molecular weight, we observed little sedimentation or bundling since the DEP field is activated before sedimentation occurs and the organic ligands on the surface of the wires provide steric stablication. These CdSe NWs have an absorption edge at ~1.8 eV (in comparison, the band gap of bulk CdSe is 1.78 eV).

The gold microelectrodes employed in this study were patterned using standard photolithography and lift-off process. Specifically, masks were used to define interdigitated electrodes with a 20–40 μm gap, and then 5 nm of titanium was sputtered onto a microscope coverslip as an adhesion layer for the subsequent evaporation of 45 nm of Au. A piece of cover well was glued above the electrodes to create an ~100 μl perfusion chamber. This prevented samples from drying too quickly during NW alignment experiments. ac electric fields with magnitudes ranging from 1 to 40 kV/cm were generated using a function generator connected to a high voltage amplifier. Corresponding ac frequencies were varied between 0.2 Hz and 10 MHz.

Fluorescence measurements, both during and after NW alignment and both in the chloroform solvent and in air, were carried out using a modified, single molecule sensitive, inverted optical microscope. The excitation source is the 488 nm line of an air cooled Ar^+ ion laser, filtered to remove any residual plasma light. The light is then passed through a polarization preserving single mode fiber to ensure a Gaussian TEM_{00} mode. It is then recollimated with a microscope objective, effectively expanding the beam's waist to ~8 mm. The orientation of the light's linear polarization is controlled using a half wave plate mounted on a rotation stage. A quarter wave plate is subsequently inserted after the $\lambda/2$ plate to create circularly polarized light for subsequent emission polarization anisotropy experiments. These experiments also involve placing an additional linear polarizer (analyzer) prior to the detector.

The microscope can be operated confocally by overfilling the back aperture of the 1.4 numerical aperture (NA) oil immersion objectives with collimated light. Alternatively, for epiillumination, an $f=250$ mm lens is inserted to focus the light prior to the objective's back aperture. This creates a wider excitation area on the sample, with a field of view reaching 30 μm in diameter. Typical excitation intensities used in our experiments range from 1 to 100 W/cm^2. Emitted light from the sample is collected with the same objective and is passed through two barrier filters to remove any excess excitation light. The emission is then imaged using either a single photon counting avalanche photodiode (Perkin Elmer SPCM AQR-14) or with a Peltier cooled charge-coupled device (CCD) (DVC 1412). More information about the apparatus can be found in Ref. 9.

Transport properties of aligned nanowires were studied through *I-V* measurements taken on an Agilent 4155B semiconductor parameter analyzer. The applied bias ranged from −40 to 40 V with obtained currents in the range of 1 pA–1 μA. Samples for these measurements were prepared by first aligning the wires between the interdigitated electrodes and letting the solvent dry with the field on. Some samples were also processed via rapid thermal annealing in order to improve the contact between the wires and the electrodes. All measurements were conducted under ambient conditions.

RESULTS AND DISCUSSIONS

In general, a number of ways exist for manipulating nanoscale objects using ac or dc electric fields.[33] For example, charged particles (or nanostructures) in solution can directly undergo electrophoresis in the presence of a uniform dc field. By contrast, nanostructures with a permanent dipole moment simply orient along the field lines due to the equal but opposing forces pulling on either side of the dipole. On the other hand, a nonuniform field can be used to manipulate neutral particles with induced and/or permanent dipoles, i.e., dielectrophoresis. In dc DEP, both permanent and induced dipoles contribute to the motion of the particle; in symmetric

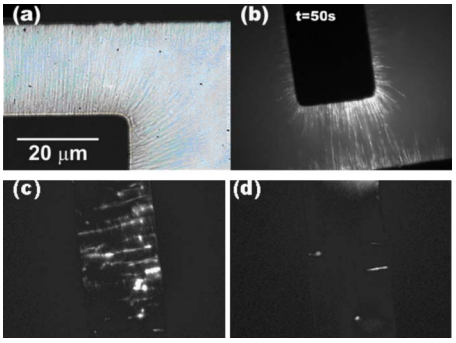

FIG. 2. Dielectrophoretically aligned CdSe NWs using an ac electric field (10 V) with electrodes separated by a 20 μm gap. [(a) and (b)] (1 MHz) Resulting bright field image after alignment and epifluorescence image taken at $t=50$ s during the alignment, respectively. [(c) and (d)] (10 kHz) Resulting alignment in 190 s, under illumination (~ 100 W/cm^2 at 488 nm) and in dark, respectively.

ac DEP, only induced dipoles contribute to the motion of the particle.[25] Specifically, when a highly polarizable, but uncharged, object such as a nanowire is subjected to an electric field, an induced dipole moment is created, enabling the object to respond to electric field gradients that are present.

In our experiments, the NWs dispersed in chloroform were observed to quickly assemble under microscope illumination between the electrodes under a reasonably strong ac electric field (>1 kV/cm) at all frequencies investigated. The alignment was detected visually through both bright field and epifluorescence measurements. Shown in Fig. 2 are aligned NWs spanning a 20 μm electrode pair. The applied ac signal had a peak voltage of 10 V, corresponding to $E_{\mathrm{rms}}=3.5$ kV/cm. Figure 2(a) is a bright field image. Apparently, the aligned NWs follow the electric field lines. Figure 2(b) shows the epifluorescence image of the same alignment under microscope illumination at $t=50$ s after the field is activated. NW assembly occurs at both electrodes as expected for a particle experiencing a positive DEP force. To illustrate the effect of super-band-gap illumination, epifluorescence images of aligned NWs were captured both under 488 nm illumination and in dark, shown in Figs. 2(c) and 2(d), respectively. It is evident that the assembly speed of CdSe NWs is much faster under illumination. In the chloroform medium ($\eta=0.58$ cP), the estimated DEP velocity is 100 μm/s under illumination compared to less than 1 μm/s in dark. These indicate that the DEP force and velocity of the NW have a strong dependence of its conductivity.

The dielectrophoretic behavior of NWs can be treated within the context of a Maxwell-Wagner formalism. If the NW and its induced dipole are not aligned with the local field, it suffers a net torque even in a spatially uniform ac field, even though there is no net translational DEP motion. As such, the rotational velocity is higher than the translational velocity by a factor that is equal to the aspect ratio of the NW, as the field gradient necessary to produce DEP translation has a length scale corresponding to the length of the NW while the dipole intensity is determined by a cross section of the NW. There is hence a rapid alignment with the field, and the subsequenct DEP motion of the NW corresponds to the one that is aligned with the local field. Both the aligned NWs and their surrounding medium can be modeled as capacitors (dielectrics) and resistors (conductors) in parallel. Dielectric polarization occurs at high frequencies when atomic dipoles form within the NW. As opposing charges of two nearby atomic dipoles cancel each other, there is no net charge within the NW at a coarsened mesoscale. A net interfacial charge exists, however, at the NW interface due to the different dielectric constants (and atomic dipole intensity) of the two media surrounding the interface. As the interfacial normal field is highest at the two ends of the NW, two localized charges of opposite sign result at the two ends to produce a dielectrically induced NW dipole. At lower frequencies, when current-carrying space charges have sufficient time to migrate to and accumulate at the two ends (if the medium conductivity is lower), a conductive polarization mechanism begins to dominate the induced dipole formation process. Hence, differences in conductivity and dielectric constant of the NW relative to its surrounding medium enable the creation of induced charges at either end of the wire in the presence of an electric field. A key ingredient of the low frequency conductive mechanism is that it requires a conducting NW with mobile charge carriers. The magnitude of the aligned induced dipole by either mechanism can be calculated using

$$\mu_{\mathrm{ind}}(t)=\varepsilon_0\varepsilon_m V_{\mathrm{NW}} K E(t), \tag{1}$$

where ε_m is the relative dielectric constant of the medium, ε_0 is the vacuum permittivity, and V_{NW} is the NW volume. K is the complex Clausius-Mossotti factor, which depends on the complex dielectric constant of the NW and that of the surrounding medium and captures both dielectric and conductive effects. Simplifying the above expression is the significantly larger longitudinal polarizability of a NW relative to its transverse (radial) polarizability. As a consequence, K for a nanowire with a corresponding Lorentz depolarization factor of $n\sim 0$ (Ref. 30) can be approximated by

$$K=\frac{(\varepsilon^*_{\mathrm{NW}}-\varepsilon^*_m)}{\varepsilon^*_m}. \tag{2a}$$

The complex dielectric constant $\varepsilon^*_{\mathrm{NW}(m)}=\varepsilon_{\mathrm{NW}(m)}\varepsilon_0 - i\sigma_{\mathrm{NW}(m)}/\omega$ of both the NW and its surrounding medium is expressed in terms of their respective conductivities, $\sigma_{\mathrm{NW}(m)}$, as well as the angular frequency of the applied field, ω. In contrast, the complex Clausius-Mossotti factor for a sphere is

$$K=\frac{\varepsilon^*_p-\varepsilon^*_m}{\varepsilon^*_p+2\varepsilon^*_m}, \tag{2b}$$

and $|K|\leqslant 1$ for all medium/particle conductivities and permittivities. As such, for high conductivity and high permittivity nanocolloids, K approaches unity at both high and low frequency limits. There is hence little sensitivity to particle conductivity or permittivity for spherical nanocolloids. The effective polarizability of NWs with larger aspect ratio, on the other hand, can be much higher than unity if either conductivity or permittivity is much higher than that of the medium.

The time-averaged dielectrophoretic force on the wire, due to the interaction between its dipole moment and the electric field gradient, can be expressed by[30]

$$F_{\mathrm{DEP}} = \mu(t) \cdot \nabla E(t) = \frac{1}{2}(\pi r^2 L)\varepsilon_m \,\mathrm{Re}\{K\}\,\nabla\,|E_{\mathrm{rms}}|^2, \qquad (3)$$

where E_{rms} is the root mean square value of the electric field and the cylinder volume is calculated using its radius r and length L. The direction of DEP motion depends on the sign of the real part of the Clausius-Mossotti factor K. This parameter captures the field-induced dielectric polarization of NW and medium atoms or molecules as well as that due to capacitive charging currents within both the NW and the medium.[34] Depending on the orientation of the dipole relative to the ac electric field as well as the permittivity and conductivity of the NW/medium, the wire can move towards either the high (positive DEP) or low (negative DEP) field region. The dielectrophoretic velocity of the NW is obtained by equating the DEP force to the viscous drag of the NW and scales as the DEP force of (3) divided by the NW length L and the medium viscosity. The DEP mobility is the factor in front of the gradient of the squared field intensity in the DEP velocity and is proportional to the real part of the Clausius-Mossotti factor K.

Equations (4) and (5) show both the high and low frequency limits of the real part of K,

$$\mathrm{Re}\{K\} = \frac{(\varepsilon_{\mathrm{NW}} - \varepsilon_m)}{\varepsilon_m} \quad (\omega \to \infty), \qquad (4)$$

$$\mathrm{Re}\{K\} = \frac{(\sigma_{\mathrm{NW}} - \sigma_m)}{\sigma_m} \quad (\omega \to 0), \qquad (5)$$

and explain why CdSe NWs in chloroform maintain a positive DEP force at all frequencies investigated. Namely, CdSe has substantial dielectric constants, $\varepsilon_{\mathrm{NW}}=10.2$ ($\varepsilon_{\perp}=9.33$, transverse direction),[16,35] and conductivities ($\sigma_{\mathrm{NW}} \sim 100\ \mu$S/cm measured for a single NW in dark)[7] relative to its surrounding medium. By contrast, chloroform has a relative dielectric constant of $\varepsilon_m=4.8$ and a corresponding conductivity of $\sigma_m=0.02\ \mu$S/cm. As a consequence, K is positive for all frequencies considered and accounts for why CdSe wires always move towards, not away from, the electrodes. It is also apparent that all nanocolloids have small DEP mobility because they cannot overcome their small volume factor $4/3\pi r^3$ for spheres in (3) by increasing its conductivity. In contrast, NWs can overcome this short dipole length limitation by increasing their conductivity as shown in (2a). As a result, conducting NWs have much higher DEP mobility than conducting spherical nanocolloids of the same volume. As seen in the NW transport properties described later in this paper, the conductivity of the NW can be easily enhanced by orders of magnitude even with moderate illumination intensity and we hence expect a corresponding increase in DEP mobility.

A positive DEP force is also observed at 10 MHz unlike common bioparticles, which transition from positive to negative DEP forces occurs at an ac crossover frequency between 100 kHz and 1 MHz.[24,33,36] That positive DEP occurs only at a relative low frequency is a problem for DEP-based sensors since the low crossover frequency makes the DEP trapping field short ranged due to double layer screening at the electrode[24] and the possibility of Faradaic reaction at the electrodes. By contrast, the 10 MHz positive DEP force seen in NWs enables the field to penetrate further into the surrounding medium. It also allows a means of separating bacteria captured by NW and those that have not docked with NW in our earlier strategy of using the high induced dipoles of nanostructures to capture pathogens.[30]

In aligned NW ensembles, we observe long-chain linear NW bundles due to dipole-dipole (end-to-end) interactions between either induced or permanent dipoles. Although permanent dipoles do not contribute to ac dielectrophoresis, they can still be responsible for the assembly. Our assembly structure is similar to those formed by single wall nanotubes (SWNTs) assembled from organic solutions.[37,38] Based on simple dipole-dipole interaction considerations, $U(r) = -\mu_1\mu_2/2\pi\varepsilon_m\varepsilon_0 r^3$, we obtain an estimated interaction potential energy between two side-to-side oriented 50 D wurtzite NW sections of ~0.5 eV (~20 kT). This assumes an interwire spacing of 1.1 nm based on the presence of TOPO ligands on NW surfaces.[39] We have also estimated that a 10 nm diameter wurtzite CdSe NW possesses an intrinsic permanent dipole moment, due to spontaneous polarization, of roughly $50L$ D, where L is the length of the nanowire expressed in nanometers. Based on conservative estimates of the spontaneous polarization for CdSe, $P \sim 0.2\ \mu\mathrm{C/cm^2}$, a 10 nm diameter wire has a total surface charge density of $\sigma_o = 1.25 \times 10^{12}\ e/\mathrm{cm^2}$. The product of this and the surface area normal to the wire growth axis gives ~1 electron per NW end face. The corresponding permanent dipole moment is then $\mu = (1.602 \times 10^{-19}\ \mathrm{C})(1 \times 10^{-9}\ \mathrm{m/nm})(L)/3.336 \times 10^{-30}\ \mathrm{C\,m/D}$ or $48L$ D for a pristine 10 nm diameter wurtzite CdSe NW, grown along the ⟨0001⟩ direction in vacuum. In the presence of mobile carriers generated by photons in the NW, a charge density will be established at either end of the nanowire during each half cycle of the ac field. To illustrate, each charge localized at the end of the wire causes a 50 000 D dipole moment in a 1 μm long NW. Therefore, a much larger interaction potential energy between NWs will result under super-band-gap illumination. Such large interaction potential energies would, in turn, suggest induced dipole-dipole interactions as the root cause of "bundling" commonly seen in NW ensembles,[2,3] which can be drastically enhanced by photon-generated charge carriers.

Additional characterization of aligned NW ensembles in air, after chloroform has evaporated, was conducted through absorption and emission polarization anisotropy measurements. In these experiments, a 1 kHz ac electric field ($E_{\mathrm{rms}}=5$ kV/cm) was first used to align the NWs, fixing their orientation by drying out the solution while keeping the field on. Figure 3 illustrates an example of NWs oriented between two electrodes. The linear polarization of the excitation was subsequently rotated using a $\lambda/2$ wave plate. Epifluorescence images of the ensemble [Figs. 3(a) and 3(b)] clearly show changes in the emission intensity with polarization angle. A movie illustrating this is also provided in the supporting information section.

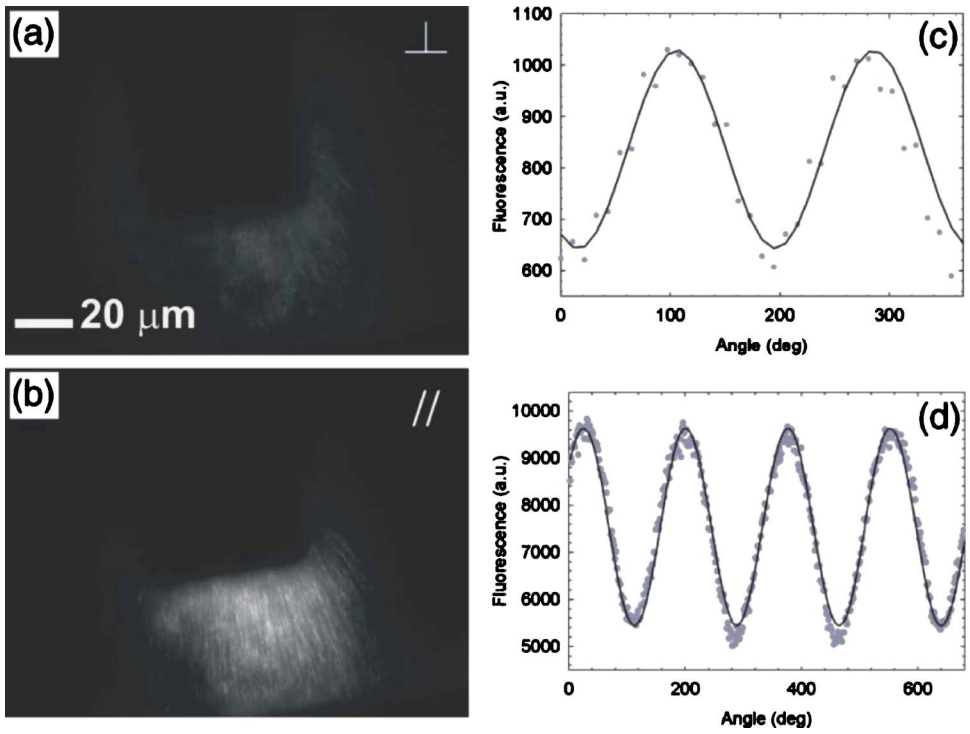

FIG. 3. (a,b) Fluorescence images from the absorption polarization anisotropy of aligned NW ensembles in air. (c) Corresponding plot of the absorption polarization anisotropy. (d) Plot of the emission polarization anisotropy from a different aligned ensemble.

Typical absorption (emission) polarization anisotropies, $\rho=(I_{\parallel}-I_{\perp})/(I_{\parallel}+I_{\perp})$, of aligned samples [$I_{\parallel(\perp)}$ are the intensities of the emitted light parallel (perpendicular) to the NW length] were determined to be $\rho\sim0.24$ (0.27) by fitting the angle dependent intensity ratio [Figs. 3(c) and 3(d)] to a $\cos^2\theta$ function. Values for the ensemble intensity were obtained by averaging intensities from seven random locations within the electrode gap. Although the results show significant net absorption/emission anisotropies, their values are suppressed relative to that seen in individual bundles as well as in individual NWs. To illustrate, rather than randomly sample the intensity in the electrode gap, if we focus only on the emission intensity from resolved bundles in the array, values of the absorption (emission) polarization anisotropy jump to $\rho=0.74$ ($\rho=0.60$). This confirms our visual observation that the actual NW dielectrophoretic alignment is incomplete despite the high degree of overall alignment (Figs. 2 and 3). Furthermore, these values are consistent with both the absorption and emission polarization anisotropies of single branched CdSe NWs seen in Fig. 4. Typical absorption (emission) polarization anisotropies from such individual NWs are found to be $\rho=0.77$ ($\rho=0.76$).

During our measurements an unusual observation was made. Namely, we observed that the electric field caused an apparent enhancement of the NW emission. More specifically, the emission intensity of aligned NWs in air, measured

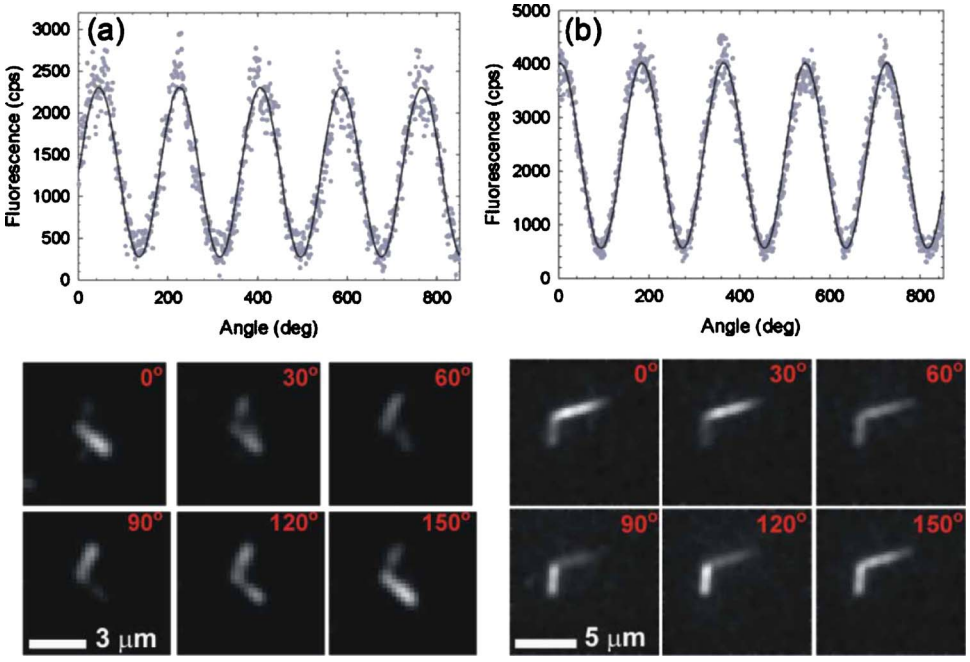

FIG. 4. (Color online) (a) Absorption and (b) emission polarization anisotropy measurements of single v-shaped CdSe NWs in air. Corresponding images of the NWs, at selected angles, are shown below.

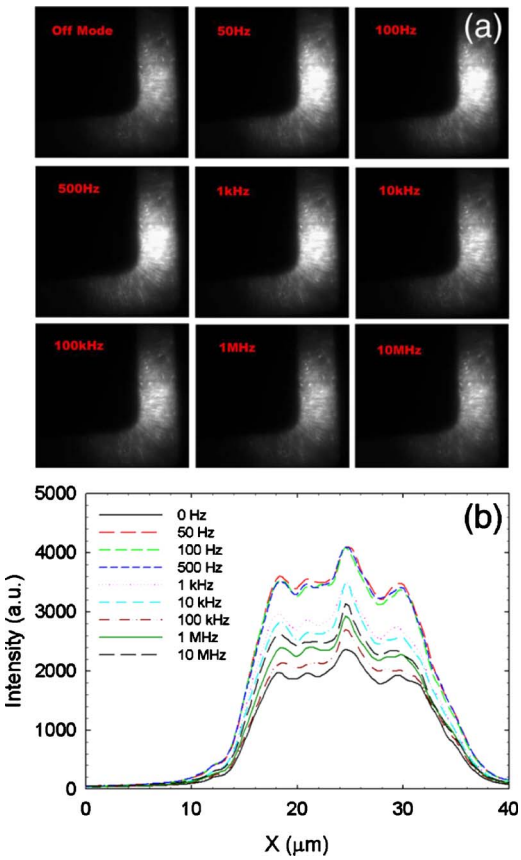

FIG. 5. (Color online) (a) Frequency-dependent fluorescence images of aligned CdSe NWs in air between 20 mm spaced electrodes. (b) Corresponding intensity cross section across the channel as a function of frequency.

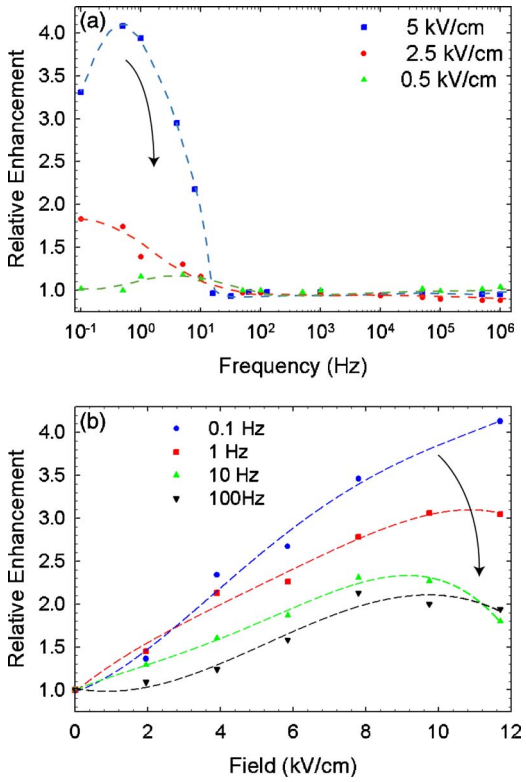

FIG. 6. (Color online) (a) Enhancements of NW emission as a function of frequency at various electric field strengths. (b) Enhancements of the NW emission as a function of electric field strength at various fixed frequencies. Dashed lines are guides to the eyes.

over a range of frequencies between 0.2 Hz and 10 MHz with an ac square wave (0.5–12 kV/cm), enhances the emission by a factor of ~4 relative to the zero field case. Figures 5(a) and 5(b) show both images and an intensity cross section of aligned NWs as a function of frequency. The applied electric field is 5 kV/cm. Visual growth in the emission intensity is apparent, following initial increases in applied ac frequency. Higher frequencies, however, cause decreases in the enhancement, which converge to the zero field value.

This trend is shown more quantitatively in Fig. 6(a), which further illustrates that the same behavior is present under different electric field strengths (0.5–5 kV/cm). In all cases, a characteristic roll-off frequency of ~10 Hz is apparent, suggesting a characteristic system response time of τ ~100 ms. Additional characterization of the phenomenon was conducted by monitoring the emission intensity while increasing the electric field strength at a given frequency. This likewise causes fluorescence enhancements up to a factor of 4. More specifically, Fig. 6(b) shows growth of the emission intensity at four fixed frequencies when field strengths are increased to 12 kV/cm. Apparent from the figure is the fact that lower ac frequencies cause the largest fluorescence enhancements in contrast to higher frequencies, which suppress the effect.

The low frequency behavior of the emission is unexpected as previous work on single NRs under dc electric fields has shown that externally applied fields generally act to reduce the electron/hole wave function overlap, causing a decrease of the overall emission intensity.[30] However, it is clear from the illumination-enhanced DEP discussion of (5) that a strong conductive current exists along the wire with a low frequency ac field. This same current vanishes under a dc field once the ends of the NW are fully charged. We hence speculate that this enhancement effect may be related to the presence of surface charges and photon-generated mobile carriers on or within the NW. These same charge carriers are responsible for the conductive currents behind illumination-enhanced induced dipoles and DEP mobility. The existence of these carriers is consistent with our recent NW FET measurements[7] as well as observed blinking phenomena in NWs.[40] The characteristic relaxation time associated with the roll-off frequency could be related to the migration time of the carriers to one end of the NW. This charge migration is the charging current responsible for the field-induced polarization and dipole formation. However, a unique charge transport mechanism must be responsible for the long time scales of nearly 100 ms. Despite our incomplete understanding of the phenomenon, the unexpected ability to enhance the emission at low frequencies and high fields offers a potentially attractive mechanism in sensing the change of surface states, thus the substance that NWs are in contact with.

In all cases, no variations of the emission spectra were observed with applied electric field. This is shown in Fig. 7 where both the field dependent emission spectra of an aligned ensemble and a single wire are shown together. While a Stark-induced redshift of the emission might be ex-

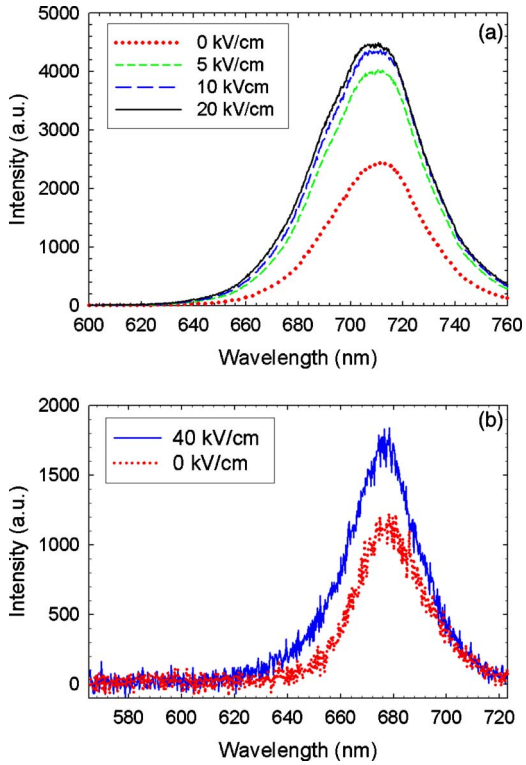

FIG. 7. (Color online) Emission spectra of (a) an aligned NW ensemble and (b) a single NW both at different electric field strengths.

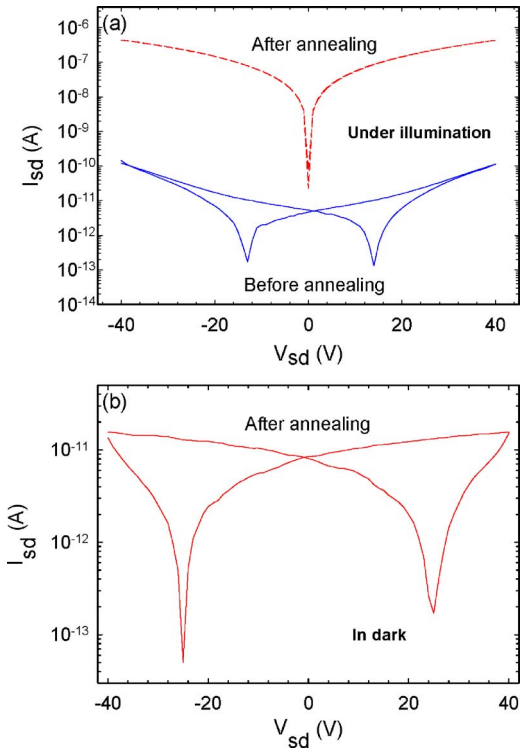

FIG. 8. (Color online) (a) Current-voltage characteristics of aligned CdSe NWs under optical illumination, both before and after rapid thermal annealing. In the latter case, a marked improvement in photocurrent is observed. (b) *I-V* characteristics of same device after annealing but without illumination.

pected, it is likely absent here because of the relatively low field strengths used in these experiments (0–40 kV/cm). In this respect, previous studies measuring the quantum confined Stark effect in semiconductor QDs have employed fields exceeding 100 kV/cm to reveal spectral shifts on the order of 10 meV.[41] Given the low fields used in our experiments, the broad emission linewidths of both ensembles and single NWs (Ref. 9) may conceal such small Stark-induced spectral shifts, leading to no apparent change of the spectrum with electric field.

To further verify that illumination generates current carriers and changes the conductivity of the wire, the electron transport properties of aligned nanowires with and without illumination were measured using an Agilent 4155B semiconductor parameter analyzer. Prior to any thermal treatment, the as-aligned CdSe nanowires on gold contact pads exhibited non-Ohmic behavior. Currents without (with) white light illumination were <10 pA (120 pA) under an average illumination intensity of ~ 540 mW/cm^2 over the spectral range between 200 and 800 nm with the larger current in the presence of light indicating the strong photoconductivity of the wires.[8] A 40 V source-drain bias was used in both cases. The low currents and non-Ohmic behavior seen in Fig. 8(a) (bottom) under optical illumination suggest poor contact between the wires and the gold electrode. This could arise from a number of reasons including the presence of surfactant on the NW surface, which acts as an insulator.

After rapid thermal annealing [1 min at 300 °C in a forming gas environment (95% N_2 5% H_2)], however, the transport properties of the aligned wires improved markedly [Fig. 8(a), top]. Ohmic behavior was observed under optical illumination and currents approached 430 nA, a three order of magnitude improvement from the previous unannealed case. Even without illumination, currents of the annealed device approached 15 pA [Fig. 8(b)]. We attribute these improvements to three factors: (a) removal of NW surface passivating surfactants that inhibit carrier flow between the nanowire and metal pads, (b) removal of surfactant between adjacent NWs in the aligned assembly, and (c) interdiffusion of Au into CdSe forming an alloyed Ohmic contact, though this remains to be verified.

CONCLUSIONS

We have shown that high aspect ratio CdSe NWs with illumination-enhanced conductivity can be manipulated using microfabricated electrodes by symmetric ac DEP. The large induced dipoles of the NWs promote their self-assembly into ordered arrays. Since super-band-gap illumination generates mobile electrons and holes, thus enhancing both the conductivity and the induced dipoles in the high aspect ratio NW, a much larger DEP mobility, thus shorter assembling time than without illumination, is observed. Absorption and emission polarization anisotropy experiments show that the NW arrays exhibit a high degree of alignment. An unexpected observation is the sensitivity of the emission to applied electric fields. Specifically a factor of ~ 4 enhancements in the emission intensity is observed at low frequencies and high fields. The illumination-sensitive DEP mobility and field-enhanced fluorescent phenomena could both be attributed to a higher conductivity due to light-generated

mobile charges. The observed strong electric-optical field coupling suggests potential uses of aligned NWs in polarization-sensitive photodetection[42] and biosensing applications. In this respect, earlier studies have shown that single viruses can be detected through NW conductivity measurements.[43] By the same token, the sensitivity of the NW fluorescence to environment and electric fields would suggest an additional means of detecting and perhaps even identifying captured pathogens, enabling future improvements in nanowire-based biosensors.

ACKNOWLEDGMENTS

Two of the authors (R.Z. and H.-C.C.) were supported by a NASA Grant No. NAG3-2701 and a NSF grant. Another author (M.K.) thanks the University of Notre Dame, the ACS Petroleum Research Fund, the NSF CAREER Program, the Notre Dame Radiation Laboratory, and the DOE Office of Basic Energy Sciences for financial support. Another author (D.J.) thanks C. Wood and Linda Chrisey C. Baatar from the Office of Naval Research for valuable discussions. Another two authors (M.K. and D.J.) also thank the Notre Dame Faculty Research Program and the Notre Dame Office of Research for financial support. One of the authors (M.K.) is a Cottrell Scholar of Research Corporation.

[1]F. Patolsky and C. M. Lieber, Mater. Today **20** (2005).
[2]H. Yu, J. Li, R. A. Loomis, P. C. Gibbons, L.-W. Wang, and W. E. Buhro, J. Am. Chem. Soc. **125**, 16168 (2003).
[3]J. W. Grebinski, K. L. Richter, J. Zhang, T. H. Kosel, and M. Kuno, J. Phys. Chem. B **108**, 9745 (2004); J. W. Grebinski, K. L. Hull, J. Zhang, T. H. Kosel, and M. Kuno, Chem. Mater. **16**, 5260 (2004).
[4]Z. A. Peng and X. G. Peng, J. Am. Chem. Soc. **124**, 3343 (2002).
[5]A. I. Mohammad and I. P. Herman, Appl. Phys. Lett. **80**, 3823 (2002).
[6]Y. Wu, H. Yan, M. Huang, B. Messer, J. H. Song, and P. Yang, Chem.-Eur. J. **8**, 1261 (2002).
[7]A. Khandelwal, D. Jena, J. W. Grebinski, K. L. Hull, and M. Kuno, J. Electron. Mater. **35**, 170 (2006).
[8]A. K. Singh, X. Li, A. Khandelwal, M. Kuno, H. Xing, and D. Jena (unpublished).
[9]V. Protasenko and M. Kuno, Adv. Mater. (Weinheim, Ger.) **17**, 2942 (2005).
[10]M. S. Gudiksen, J. Wang, and C. M. Lieber, J. Phys. Chem. B **105**, 4062 (2001).
[11]R. Krupke, F. Hennrich, H. V. Lohneysen, and M. M. Kappes, Science **301**, 344 (2003).
[12]A. P. Alivisatos, J. Phys. Chem. **100**, 13226 (1996); J. T. Hu, L. S. Li, W. D. Yang, L. Manna, L. W. Wang, and A. P. Alivisatos, Science **292**, 2060 (2001).
[13]A. Shabaev and Al L. Efros, Nano Lett. **4**, 1821 (2004).
[14]I. Robel, B. Bunker, P. Kamat, and M. Kuno, Nano Lett. **6**, 1344 (2006).
[15]E. A. Muljarov, E. A. Zhukov, V. S. Dneprovskii, and Y. Masumoto, Phys. Rev. B **62**, 7420 (2000).
[16]L.-S. Li and A. P. Alivisatos, Phys. Rev. Lett. **90**, 097402 (2003).
[17]T. Nann and J. Schneider, Chem. Phys. Lett. **384**, 150 (2004).
[18]M. E. Schmidt, S. A. Blanton, M. A. Hines, and P. Guyot-Sionnest, J. Chem. Phys. **106**, 5254 (1997).
[19]F. Bernardini, V. Fiorentini, and D. Vanderbilt, Phys. Rev. B **56**, R10024 (1997).
[20]P. A. Smith, C. D. Nordquist, T. N. Jackson, T. S. Mayer, B. J. Martin, J. Mbindyo, and T. E. Mallouk, Appl. Phys. Lett. **77**, 1399 (2000).
[21]D. Whang, S. Jin, and C. M. Lieber, Nano Lett. **3**, 951 (2003); J. Appl. Phys. **43**, 4465 (2004).
[22]A. Tao, F. Kim, C. Hess, J. Goldberger, R. He, Y. Sun, Y. Xia, and P. Yang, Nano Lett. **3**, 1229 (2003).
[23]S. Acharya, A. B. Panda, N. Belman, S. Efrima, and Y. Golan, Adv. Mater. (Weinheim, Ger.) **18**, 210 (2006).
[24]R. Zhou, P. Wang, and H.-C. Chang, Electrophoresis **27**, 1376 (2006).
[25]Y. Huang, X. Duan, Q. Wei, and C. M. Lieber, Science **291**, 630 (2001).
[26]K. Yamamoto, S. Akita, and Y. Nakayama, J. Phys. D **31**, L31 (1998).
[27]R. Krupke, F. Hennrich, H. Lohneysen, and M. Kappes, Science **301**, 344 (2003).
[28]M. Dimaki and P. Boggild, Phys. Status Solidi A **203**, 1088 (2006).
[29]E. Rothenberg, M. Kazes, E. Shaviv, and U. Banin, Nano Lett. **5**, 1581 (2005).
[30]J. J. Boote and S. D. Evans, Nanotechnology **9**, 1500 (2005).
[31]K. L. Hull, J. W. Grebinski, T. H. Kosel, and M. Kuno, Chem. Mater. **17**, 4416 (2005).
[32]M. Kuno, O. Ahmad, V. Protasenko, D. Bacinello, and T. Kosel, Chem. Mater. **18**, 5722 (2006).
[33]H. A. Pohl, *Dielectrophoresis* (Cambridge University Press, Cambridge, 1978).
[34]J. Wu, Y. Ben, D. Battigelli, and H.-C. Chang, Ind. Eng. Chem. Res. **44**, 2815 (2005).
[35]*Semiconductors: Other than Group IV Elements and III-V Compounds*, edited by O. Madelung (Springer, New York, 1992), p. 29.
[36]Z. Gagnon and H.-C. Chang, Electrophoresis **26**, 3725 (2005).
[37]P. V. Kamat, G. Thomas, S. Barazzouk, G. Grishkumar, V. Vinodgopal, and D. Meisel, J. Am. Chem. Soc. **126**, 10757 (2004).
[38]X. Q. Chen and T. Saito, Appl. Phys. Lett. **78**, 3714 (2001).
[39]C. R. Kagan, C. B. Murray, and M. G. Bawendi, Phys. Rev. B **54**, 8633 (1996).
[40]M. Kuno (private communication).
[41]S. A. Empedocles and M. G. Bawendi, Science **278**, 2114 (1997).
[42]A. Singh, A. Khandelwal, X. Li, H. Xing, M. Kuno, and D. Jena, Digest of Device Research Conference, Pennsylvania State University, PA, June 2006 (unpublished).
[43]F. Patolsky, G. Zheng, O. Hayden, M. Lakadamyali, X. Zhuang, and C. M. Lieber, Proc. Natl. Acad. Sci. U.S.A. **101**, 14017 (2004).